

## Molecular dynamics simulations of electrophoresis of polyelectrolytes in nano confining cylindrical geometries

S. Nedelcu and J.-U. Sommer

Citation: *The Journal of Chemical Physics* **138**, 104905 (2013); doi: 10.1063/1.4794195

View online: <http://dx.doi.org/10.1063/1.4794195>

View Table of Contents: <http://scitation.aip.org/content/aip/journal/jcp/138/10?ver=pdfcov>

Published by the [AIP Publishing](#)

---

### Articles you may be interested in

[Brownian dynamics simulations of polyelectrolyte molecules traveling through an entropic trap array during electrophoresis](#)

*J. Chem. Phys.* **127**, 124902 (2007); 10.1063/1.2777157

[Electrophoretic properties of highly charged colloids: A hybrid molecular dynamics/lattice Boltzmann simulation study](#)

*J. Chem. Phys.* **126**, 064907 (2007); 10.1063/1.2431174

[Molecular dynamics simulation of the polymer electrolyte poly\(ethylene oxide\)/ Li Cl O 4 . II. Dynamical properties](#)

*J. Chem. Phys.* **125**, 214903 (2006); 10.1063/1.2400221

[Dynamics of poly\(ethylene oxide\) in nanoscale confinements: A computer simulations perspective](#)

*J. Chem. Phys.* **118**, 3421 (2003); 10.1063/1.1538601

[Molecular dynamics simulation of interfacial electrolyte behaviors in nanoscale cylindrical pores](#)

*J. Chem. Phys.* **117**, 5850 (2002); 10.1063/1.1501585

---



## Re-register for Table of Content Alerts

Create a profile.



Sign up today!



# Molecular dynamics simulations of electrophoresis of polyelectrolytes in nano confining cylindrical geometries

S. Nedelcu<sup>1,a)</sup> and J.-U. Sommer<sup>1,2,3,b)</sup>

<sup>1</sup>Leibniz-Institut für Polymerforschung Dresden e.V., Hohe Strasse 6, Dresden D-01069, Germany

<sup>2</sup>Technische Universität Dresden, Dresden D-01069 Germany

<sup>3</sup>Institute for Theoretical Physics, Technische Universität Dresden, Zellescher Weg 17, D-01069 Dresden, Germany

(Received 20 December 2012; accepted 13 February 2013; published online 13 March 2013)

We consider molecular dynamics simulations of the electrophoretic motion of charged polymers in straight cylinders and cylinders with a periodic variation (or modulation) of the diameter. The electric field is always orientated along the axis of the cylinders, and it does not change direction. The fluid is modeled explicitly, also the co-ions, counterions, and the charged polymer monomers. In straight geometries, we observe no separation effect for a wide range of applied electric fields. In modulated geometries, the charged polymer chains can be separated only at low fields. At large fields, we observe separation effects in modulated geometries only if the applied field is a dc pulse electric field. A simple scaling theory to explain the observed behavior is presented. © 2013 American Institute of Physics. [<http://dx.doi.org/10.1063/1.4794195>]

## I. INTRODUCTION

The migration of charged polymer chains under the influence of electric fields in solution is a complex transport problem of high interest in the field of biotechnology, and separation science technology. The history of the subject spans several decades, starting with capillary zone electrophoresis experiments, and subsequent improvements by using alternating fields,<sup>1,2</sup> to more recent advances using nanoscale devices.<sup>3–12</sup> As repeatedly observed in electrophoresis experiments in free solution, charged polymer chains driven by external constant fields move with electrophoretic velocities independent of the chain length.<sup>13</sup> This is a consequence of the balance between forces of electric origin, which are long-range Coulomb interactions between the charged chains and the co-ions and counterions present in solution, and hydrodynamic forces (also long range) due to the solvent.<sup>14</sup> In particular, for distances larger than Debye length, the hydrodynamic forces are generally assumed to be screened, while inside the Debye layer, the electric driving force is almost balanced by the electroosmotic flow of the counterions.<sup>15</sup> The full analytical solution of the electrophoretic transport has been obtained before for charged colloidal particles in laminar flow, but electrokinetic solutions for flexible charged chains, in arbitrary environments, still remain challenging and can be obtained only numerically.<sup>16</sup>

In the present molecular dynamics simulations, we consider the electrophoresis of charged chains in free solution in confining straight cylinder geometries and cylinders with a periodic modulation of the diameter (Fig. 1). The applied electric field is always along the cylinder axis and can be constant, or square pulse field. Pressure-driven flow experiments reporting length- and topology-dependent separation but for

a slit-well geometry (or nanogroove arrays) are reported for example by Mikkelsen *et al.*<sup>17</sup>

As it is known from electrophoresis in free solution, charged chains are able to change shape by folding, extending, contracting, tying themselves into knots, etc. Since the hydrodynamic friction depends on the chain shape and the electro-osmotic flow within the Debye layer,<sup>18,19</sup> the modulated geometries allow us to control these factors and ultimately to separate the chains by size. Specifically, we consider two chain lengths  $N = 70$  and  $N = 150$ . We choose the size and shape of the cavities such that at equilibrium, the  $N = 70$  chain can be entirely contained in one single cavity, while the chain with  $N = 150$  monomers spans two cavities (Fig. 2). The constrictions between cavities act as potential barriers (see, for example, Slater's work in Ref. 20). When the applied field is turned on, and maintained constant, the short chain moves forward by successive jumps, from one cavity to the next. In contrast, the longer chain has a smoother motion since it always extends on two cavities, which makes the potential barriers appear lower. As a result of different heights of the barriers, the chains move with different velocities, and therefore can be separated. In these type of experiments, the diffusion processes, which are chain length dependent, play no role. It is thus not surprising that at high fields, when the potential barriers become next to negligible, both chains move with equal velocities. When the constant applied field is changed from a constant field into a pulse field, the diffusion effects become important and charged chains can again be separated, as we shall discuss below. The full process is therefore a combination of forces due to polymer elasticity, diffusion, and barrier potentials.

We note here that our final aim is to obtain the passage of the chains through constrictions dependent on chain length even at high electrophoretic velocities. This process may depend on the particular shape of the constriction and also on the

<sup>a)</sup>Electronic mail: nedelcu@ipfdd.de.

<sup>b)</sup>Electronic mail: sommer@ipfdd.de.

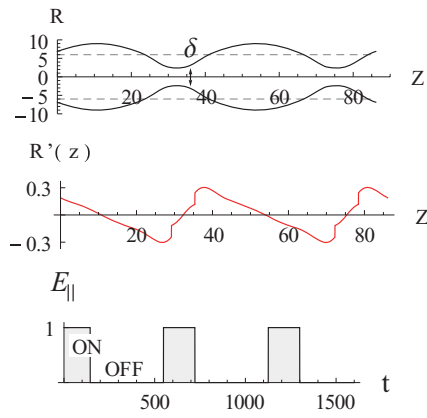


FIG. 1. (Top) Schematic cross-section of (dashed) constant, and (black) periodically modulated diameter cylinders. (Middle) The corresponding surface gradient  $R'(z)$  as a function of  $z$ -coordinate. (Bottom) The driving pulse electric field of maximum amplitude  $E_{\parallel}$  as a function of time. The off-time window takes 70% of a time period  $T = 578\tau$ .  $\delta$  notes the diameter of the constriction.

length of the on-off time windows of the applied electric field. These, however are very complex issues, and for the case of applied pulse fields, we investigate only a restricted, proof-of-concept setup, where the off-time window of the field takes 70% of a time period. For the case of constant applied electric fields, we fit our simulation results to a proposed scaling theory. When the applied fields are of pulse type (mixed biased diffusion and free diffusion), the scaling theory is augmented to account for the relaxation of the chains during the off-time window of the applied electric field.

## II. METHOD

The polymers in the simulations are bead-spring models where each monomer interacts with its connected neighbors through a finite-extensibility-nonlinear-elastic (FENE) potential

$$U_{FENE} = -kR_0^2 \log(1 - (r/R_0)^2), \quad (1)$$

where  $k = 30$ ,  $R_0 = 3\sigma$  is the maximum extension of the bond,  $r$  is the distance between beads, plus a short-range Lennard-Jones potential

$$U_{LJ} = \epsilon \left( \left( \frac{\sigma}{r} \right)^{12} - \left( \frac{\sigma}{r} \right)^6 \right), \quad (2)$$

where  $\epsilon$  and  $\sigma$  are the unit energy and unit length, respectively. We use a cutoff for the LJ potential at  $\sqrt{2}\sigma$  and a shift to retain only the repulsive part of the potential. Additionally,

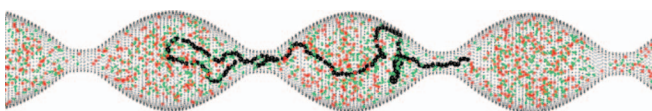


FIG. 2. Illustration of a sample configuration from molecular dynamics simulations of (black) charged polymer chain of length  $N = 150$ , (green) coions and (red) counterions in confining cylinder of variable diameter. The chain extends on two neighboring cavities and passes through constrictions by forming loops. (The direction of motion is from right to left.) For clarity, the solvent molecules are not represented here.

we add an angle harmonic potential  $K(\theta - \theta_0)^2$  between adjacent bonds, where  $K = 100$  and  $\theta_0 = 145^\circ$ . The stiffness of the chain is introduced with the intent to make one chain span two cavities. If the polymer chains are less stiffer, then the size of the cavities is to be adjusted accordingly, in the sense that these must be made smaller. Each chain monomer carries a negative electric charge and interacts with co-ions and counterions through long-ranged Coulomb potential

$$U_C = \frac{1}{4\pi\epsilon\epsilon_0} \frac{q_i q_j}{r^2}, \quad (3)$$

where  $q_i$  is the charge and  $\epsilon = 80$  is the dielectric constant of the solvent.

The fluid is modeled explicitly by neutral beads, which interact with each other through LJ forces. The monomer number density of the fluid monomers is set at  $0.82\sigma^{-3}$ . The particles are restricted to the interior of a cylinder of constant, or variable diameter and can only leave, and enter the simulation box in the  $z$ -direction. The 3D-shape of the modulated diameter cylinder is obtained by a revolution about  $z$ -axis of the curve  $-1.5|\text{Sin}[c]|^9 + |\text{Cos}[2c] + 0.9|$ , where  $c = 0.146(z - 26.9)$ . Hence, the diameter of the modulated cylinder varies between  $4.8\sigma$  and  $18\sigma$ . As a comparison, the average bond length of the polymer chain is  $\approx 1.15\sigma$ , and the straight cylinder diameter is  $12\sigma$ . In the  $x=$  and  $y=$  directions, the size of the simulation box is a few times larger than the largest diameter of the cylinder. This assures that the electrostatic interactions, which are calculated using 3D periodic boundary conditions and Ewald summation method, are negligible in these directions. We built the cylinder surface using neutral monomers, which interact through LJ forces with the fluid and the polymer chains. The surface is relatively closely packed such that no fluid monomers can leave the cylinder in the  $x=$ , or  $y=$  direction. To possibly enhance the separation resolution at the edges of the connecting channels, we introduced slight steps, which can be seen from the drop in  $R'(z)$  in Fig. 1.

The number of counterions in the volume of the simulation box is of the order of thousands and gives a Debye length of  $\lambda_D = \sqrt{2z^2 e^2 n_\infty / \epsilon k_B T} = 4.75\sigma$ . For comparison, the gyration radius of the chain with  $N = 70$  monomers when the cylinder walls are removed is  $R_g(N = 70) \approx 11.78\sigma$ . This places the Debye layer thickness in the lower thin layer limit, since  $\lambda_D^{-1} R_g(N = 70) \approx 2.48$  is not much larger than unity.

The simulations were carried out separately for each chain length using LAMMPS (<http://lammps.sandia.gov>), and in particular the CUDA-USER package for accelerating the calculation of the electrostatic interactions using graphical processing units. The ensemble used is canonical (NVT) with a Nose-Hoover thermostat,<sup>21</sup> at a reduced temperature of  $3k_b T/\epsilon$ . The time step used in the simulations is  $\Delta t = 0.008\tau$ , where  $\tau$  is the unit LJ time.

## III. RESULTS AND DISCUSSIONS

In a classical straight cylinder, of uniform diameter, the polyelectrolytes move with electrophoretic velocities  $v_z$  independent of  $N$  for much of the interval of the applied electric fields (Fig. 3). This type of geometry serves only as a refer-

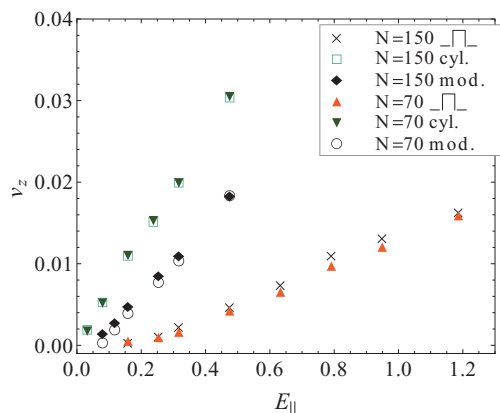


FIG. 3. Electrophoretic velocities  $v_z$  of charged chains of length  $N$  as a function of the applied field  $E_{\parallel}$  in uniform (noted cyl.) and modulated (noted mod.) diameter cylinders, and in modulated cylinders under pulse field of amplitude  $E_{\parallel}$  (noted  $\square$ - $\triangle$ ). The error bars are smaller than the symbol size. (The off-time window of the pulse field is 70% of a time period.)

ence, since we aim to distinguish between the two test charged chains when they travel at higher velocities. By introducing a periodic modification of the diameter of the cylinder along the main axis, we introduce in effect a periodic energetic potential barrier in the  $z$ -direction, which results in electrophoretic velocities dependent on  $N$  at low field values, and independent of  $N$  at larger fields. The differences in chain velocities shown in Fig. 3 are better emphasized in Fig. 4, which shows for a few particular cases the average positions after an elapsed set time of the applied electric field.

Considering yet the modified geometry under constant applied fields, the range of low values is where the short chain motion appears discontinuous, made of fast jumps with velocity  $v_t$  from one cavity to the next (Fig. 5). The jumps are interleaved with stationary positions located at the center of the cavities, which take a time of the order of  $t_b$  (Fig. 5). At larger applied fields, the potential energy barriers are reduced and the time  $t_b$  spent by the chains in cavities becomes negligible, as we shall discuss in Sec. IV. Consequently, both short

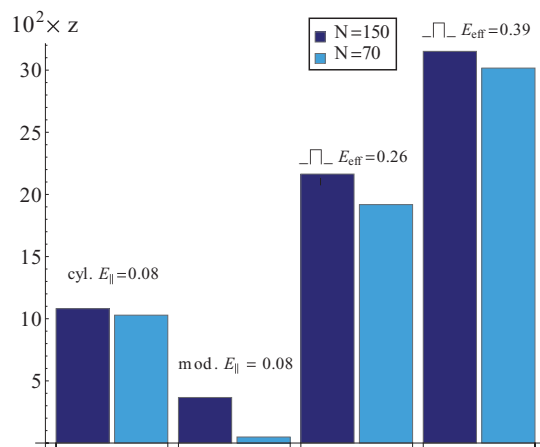


FIG. 4. Bar diagram of average positions  $z$  after a set time interval of electrophoresis of charged chains of length  $N$  in constant (noted cyl.) and variable diameter (noted mod.) cylinders under constant applied fields  $E_{\parallel}$ , and similar positions in modulated cylinders (noted  $\square$ - $\triangle$ ) in applied pulse fields of relative strength  $E_{eff}(=E_{\parallel}/3)$ .

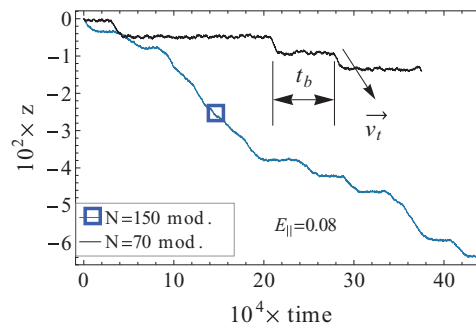


FIG. 5. Schematic illustration on the center of mass motion  $z = z(t)$ , at constant low fields  $E_{\parallel} = 0.08$ , of the trapping time  $t_b$  of charged chains in the cavities of modulated diameter cylinders and the transit velocity  $v_t$  through constrictions.

and long chains move at high fields with the same velocity (Fig. 3). As compared with the constant diameter cylinder, the modified geometry proves therefore to be successful, at least from the point of view of the separation resolution, since now chains can be distinguishable even if they move with higher electrophoretic velocities.

We keep the modified cylinder geometry and exchange the constant applied field for a pulse field. The square pulse field is simply a succession of on/off-time windows during which the chains are periodically driven through and let to relax to equilibrium. If the effect of constrictions on the electrophoretic motion is reflected by the parameters  $t_b$  and  $v_t$ , then for the case of pulse fields, the effect of relaxation can be seen on the trajectory of the center of mass as a backtrack motion (Fig. 6). The mixing of biased diffusion with free diffusion results therefore in a strong coupling between electrophoretic velocity, chain elasticity, and external potential. The electrophoretic velocity is then chain-length dependent for a larger interval of applied fields. Just as for the two cases discussed above, it becomes independent of chain length at very large electric fields (Fig. 3).

We consider briefly hydrodynamic effects. If a long polymer chain had been a solid object, such as, for example, a cylinder with rounded tops, we could possibly use classical formulas to estimate the hydrodynamic resistance met by the charged chain during electrophoretic motion. These classical

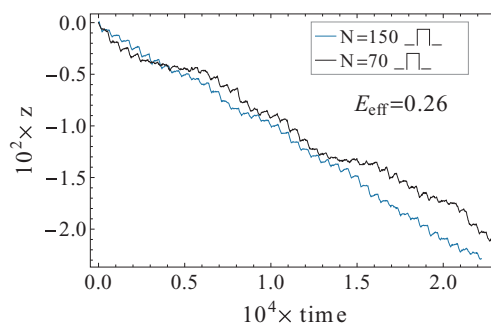


FIG. 6. Illustrative trajectories at small time scale of the center of mass motion of charged chains in modulated diameter cylinders under pulse electric fields. The relaxation (or free diffusion) of the chains in the off-time window of the pulse field appears as a backtrack motion and makes the trajectories appear zigzagged.

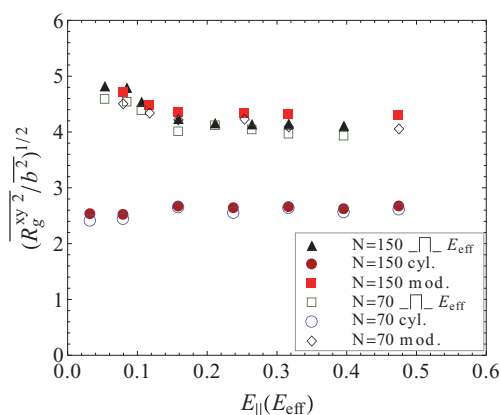


FIG. 7. The long time average of the transverse radius of the chain normalized by the bond length  $b$  as a function of constant applied field  $E_{||}$  in constant (noted cyl.), variable diameter cylinders (noted mod.), and in pulsed fields (noted  $\square$ ). The error bars are smaller than the symbol size. (In the case of pulse fields,  $E_{||}$  is rescaled by a factor of  $1/3$  to account for the off-time window of a time period.)

formula in their simplest form would require as input simple information about the object, such as cylinder radius and axial length, assuming that the cylinder is more or less aligned with the driving force during motion. The hydrodynamic friction would then be proportional with the product of fluid viscosity, square of the radius, and axial length.

However, as noted above, the charged chains are not solid objects, but rather flexible and because of the confinement solvent monomers must flow not only around the charged chains, as in Zimm's hydrodynamic model,<sup>22</sup> but also through the charged polymer coils. The porous nature (from a hydrodynamic point of view) of the polymer coil renders therefore inapplicable the classical formula for hydrodynamic resistance.

To have at least a qualitative measure of hydrodynamic resistance, we can nevertheless use the gyration tensor. Since the confining geometry is cylindrical, the flexible chains must assume a cylindrical shape. We use the  $x$  and  $y$  components of the gyration tensor,  $R_g^x$  and, respectively,  $R_g^y$ , to define the chain radius  $\sqrt{R_g^{xy}} = \sqrt{R_g^x + R_g^y}$  (Fig. 7). We may also call this the transverse radius, because it is measured in a plane perpendicular to the symmetry axis of the cylindrical geometry. We define the length of the chain as the average extension of the chain in the  $z$ -direction. The extension is noted with  $|z_{max} - z_{min}|$ , and is a time average value, where  $z_{max}$  and  $z_{min}$  are the  $z$ -coordinates of the rightmost and, respectively, leftmost  $z$ -coordinates of chain monomers (Fig. 8). As defined, the chain  $z$ -extension is not the same as the classical end-to-end distance, which is the average distance between the first and the last monomer of the chain.

We consider first the straight cylinder geometry and constant applied electric fields. The transverse radii  $R_g^{xy}$  of the two chains are similar, and nearly constant for the full range of applied fields. The  $z$ -extension of the chains does, however, change with the applied electric field. At low fields,  $|z_{max} - z_{min}|$  has the largest value and then decreases as the field increases. The decrease in the  $z$ -extension of the chains may seem counter-intuitive, and indicates that the chains compress themselves into more compact shapes as they travel

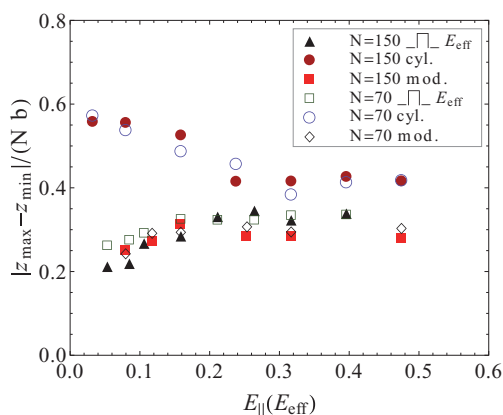


FIG. 8. Projected length  $|z_{max} - z_{min}|$  in the field direction normalized by the contour length  $Nb$  of the chains. The legend notation is the same as in Fig. 7. The error bars are smaller than the symbol size.

faster at high fields. The effect is purely hydrodynamic. Further, if we assume that the driving force of the chains increase in the same ratio as their contour lengths, and noting from Fig. 8 that  $|z_{max} - z_{min}| \approx N$ , it follows that the electric driving force is perfectly balanced by hydrodynamic friction. The end result, as noted above, is that the chains move with the same electrophoretic velocity at high fields.

Second, we consider the modulated geometries and constant applied fields. Here, the chains thread through constrictions, which have smaller diameter than the diameter of the expansion chambers, and therefore the long time averages of  $R_g^{xy}$  can be larger than the radius of the straight cylinders, which is in between the two values (Fig. 1). The transverse radii decrease slightly with increasing field, up to  $E_{||} \approx 0.2$ . This effect indicates a preferential orientation of the chains in the field direction, with increasing velocities. This has the result that  $|z_{max} - z_{min}|$  also increases (Fig. 8). This behavior is quite dissimilar to the case of electrophoresis in constant diameter cylinders, and is simply a consequence of the physical barriers posed by the constrictions, because the narrow connecting channels between the cavities force a preferential orientation of the chains as they pass through. At low fields, the reorientation processes coupled with the fact that the trapping time in the cavities depends on chain length  $N$  leads to electrophoretic velocities dependent on  $N$ . At high fields, the barrier effect is much reduced, as shown for example by the transit velocities (Fig. 9), and finally both chains move with similar electrophoretic velocities.

Finally, we consider the case of variable-diameter cylinders and applied pulse fields. We note that both the transverse radii and the  $z$ -extensions are qualitatively similar to the case of modulated cylinders and constant applied fields. There are, however, additional relaxation effects during the off-time window of the applied field that must be taken into account. These relaxation effects are inherently chain-length dependent, which lead to separation by size of the polyelectrolytes at fields as high as  $E_{||} = 0.8$  (Fig. 3). Beyond this field value, which is particular to the present setup, the relaxation effects have a diminishing impact on the electrophoretic motion, and the chains move with the same velocity.

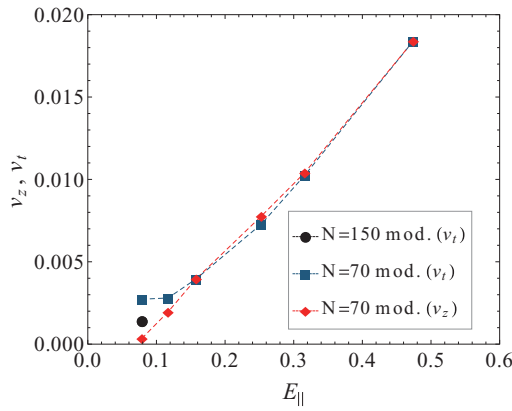


FIG. 9. Transit velocities  $v_t$  and average electrophoretic velocities  $v_z$  of the charged chains driven in modulated diameter cylinders as a function of the applied field  $E_{\parallel}$  (not pulse field). At high fields, both  $v_t$  and  $v_z$  coincide. The largest chain of  $N = 150$  passes through constrictions almost unhindered, at fields  $E_{\parallel} > 0.08$ .

#### IV. SCALING THEORY

We present in the following a scaling theory for the trapping time  $t_b$  of the shortest chain as a function of the applied electric field  $E_{\parallel}$ . For the purpose of clarity, we reduce the cavities (Fig. 2) to simplified cylinders of uniform diameter  $R_0$  and the connecting channels to cylinders of uniform diameter  $\delta$  (Fig. 10).

Here, we consider that at equilibrium and in the absence of the applied field, the chain can be entirely contained into one cavity. The migration of the charged chain as a function of the applied electric field can then be divided into three regimes.<sup>23</sup>

The first migration regime is at low applied electric fields when the chain is in equilibrium in a cavity, without entering the connecting channel yet. The energy barrier is simply the sum of entropic and electric free energies. To derive these two expressions, we consider a compression blob model of the chain, where the number of monomers in a compression blob is  $g \sim (\Omega/(Na^3))^{1/(3\nu-1)}$ , where  $a$  is the bond length. The entropic free energy due to volume interactions is

then

$$F_{ent} \sim k_B T ((N^{\nu} a^3) / \Omega)^{1/(3\nu-1)} \quad (4)$$

and the electric free energy contribution is

$$F_{elec} \sim N q e E_{\parallel} L, \quad (5)$$

where  $L$  is the chain projection in the  $z$ -direction. The effective charge of the chain is assumed to be equal to the bare charge, which is the case when counterion condensation effects are negligible. The maximum barrier potential is attained when the total free energy  $F_{ent} + F_{elec}$  is at a maximum. Solving  $\partial(F_{ent} + F_{elec})/\partial L = 0$  for  $L$  it follows that  $L^* = (k_B T)^{(3\nu-1)/3\nu} N^{(1/3\nu)} R_0^{-2/3\nu} (q e E_{\parallel})^{(1-3\nu)/3\nu}$  and the equilibrium number of monomers in a compression blob

$$g^* \sim (q e E_{\parallel} a / (k_B T) N a^2 / R_0^2)^{-1/(3\nu)}. \quad (6)$$

In the second regime, at higher applied electric fields, the chain penetrates into the connecting channel. We note with  $x$  the position of the first monomer/blob of the chains and with  $n$  the numbers of chain monomers in the connecting channel. In this regime, we assume that the size of the compression blobs is the same as  $\delta$ , the diameter of the connecting cylinder (Fig. 10). The entropic energy per monomer after entry is  $\sim k_B T / g_{in}$ , where  $g_{in} \sim (\delta/a)^{1/\nu}$ , and the free energy per monomer behind the channel is  $k_B T / g^*$ . Similarly, the electric contribution to the total free energy is  $\sim -n q e E_{\parallel} x$ . It is important to note here that the field inside the connecting channel is assumed to be unperturbed from the field in the cavity (the channel walls are assumed electrically non-conducting). The total free energy can therefore be written as following:<sup>24</sup>

$$\Delta F \sim k_B T (1/g_{in} - 1/g^*) (g_{in}/\delta) x - q e E_{\parallel} (g_{in}/\delta) x^2, \quad (7)$$

where  $x = (n/g_{in})\delta$ . The height of the potential barrier  $\Delta U$  appears at  $x = x^*$  and results from the condition of maximum of the total free energy  $\Delta F$ :

$$\Delta U \sim (k_B T)^2 / (q e E_{\parallel} (\delta/g_{in})) (1/g_{in} - 1/g^*)^2. \quad (8)$$

From Eq. (8), it is noted that the entry barrier depends on the chain length and decreases with increasing chain length.<sup>24</sup>

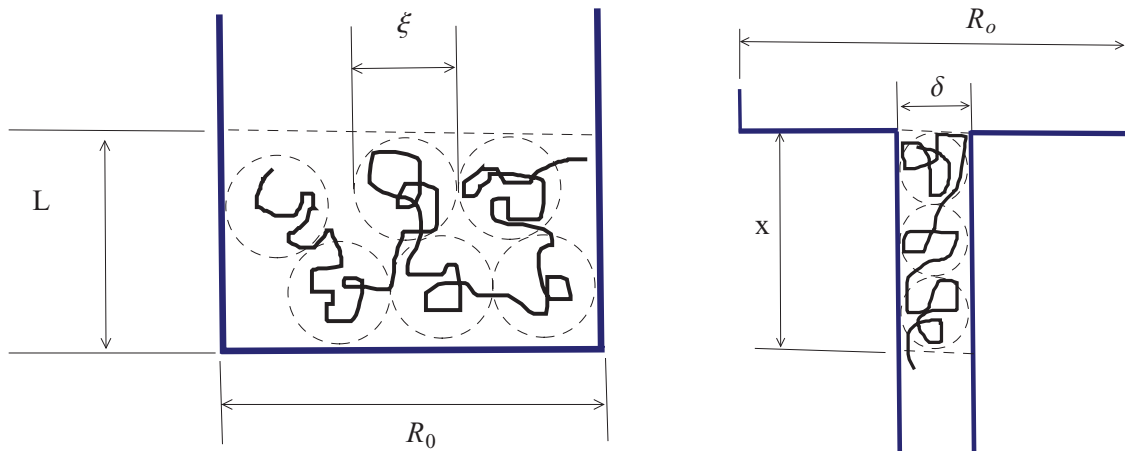


FIG. 10. (Left) Schematic representation of a compression blob model of a chain squeezed in a cylindrical confining cavity of diameter  $R_0$ . At equilibrium between forces of entropic and electric origin, the chain occupies the confined volume  $\Omega = L R_0^2$ . (Right) At higher applied electric fields,  $n$  monomers of the chain are pushed into the connecting channel of diameter  $\delta$  for a distance  $x$ .

The trapping time, or the escape time  $\tau$  of the chain which passes from one cavity to the next by surmounting the potential barrier  $\Delta U$  can be obtained by solving the one-dimensional Fokker-Planck equation<sup>25,26</sup> for the potential  $F(x)$  given in Eq. (7):

$$\frac{\partial P(x, t)}{\partial t} = \frac{\partial}{\partial x} \frac{1}{\gamma(x)} \left[ \frac{\partial F(x)}{\partial x} + \frac{\partial}{\partial x} k_B T \right] P(x, t), \quad (9)$$

where  $\gamma(x) = \eta x$  is the  $x$ -dependent friction coefficient.<sup>23</sup> The solution of Eq. (9), with reflective boundary at  $x = 0$  and absorbing boundary at  $x = x_0 \gg x^*$  (here,  $x^*$  is the position inside the channel where the total free energy Eq. (7) is at maximum) can be written as following:<sup>23</sup>

$$\tau = \int_0^{x_0} dx \cdot x \cdot e^{\frac{\Delta F(x)}{k_B T}} \int_0^x dx' \frac{1}{x' D(x')} e^{-\frac{\Delta F(x')}{k_B T}}, \quad (10)$$

where  $D(x) \simeq k_B T / \gamma(x)$ . Using the short notation

$$\Delta F / (k_B T) = Ax - Bx^2, \quad (11)$$

where

$$A = \frac{1}{\delta} \left[ 1 - \left( \frac{\delta}{a} \right)^{1/\nu} \left( \frac{qeE_{\parallel} a}{k_B T} \cdot \frac{Na^2}{R_0^2} \right)^{1/(3\nu)} \right] \quad (12)$$

and

$$B = \frac{qeE_{\parallel}}{k_B T \delta} \cdot \left( \frac{\delta}{a} \right)^{1/\nu}, \quad (13)$$

then the last integral in Eq. (10) can be greatly simplified considering that the term  $\exp(-\Delta F(x')/(k_B T))$  is very small at  $x^* = A/(2B)$  and thus

$$\int_0^{x^*} e^{-Ax' + Bx'^2} dx' = \frac{\sqrt{\pi}}{2} \frac{1}{\sqrt{B}}. \quad (14)$$

This term is a constant, which can be taken out of the first integral in Eq. (10). On the other hand, this integral is sharply peaked at  $x^*$  and it can be simplified to the following relation:

$$\int_0^{x_0} x e^{Ax - Bx^2} dx = \frac{\sqrt{\pi}}{2} \frac{1}{\sqrt{B}} x^* \cdot e^{\Delta U / (k_B T)}. \quad (15)$$

The final expression for the mean escape time  $\tau$  is then:

$$\tau \sim \frac{\eta}{k_B T} \frac{x^*}{B} e^{\Delta U / (k_B T)} \sim \frac{\eta}{k_B T} \frac{A}{B^2} e^{A^2 / (4B)}. \quad (16)$$

We are reminded here that Eq. (16) is valid if the size of a cavity is larger than  $\Omega$ , and the diameter  $\delta$  of the connecting channels is sufficiently large that a blob theory can be formulated. It is also assumed that the size  $\xi$  of a compression blob is independent of chain length  $N$ . The height of the potential barrier  $\Delta U$  is larger than the thermal energy, i.e.,  $\Delta U \gg k_B T$ , which after using Eqs. (6) and (8) reduces to the inequality  $qeE_{\parallel} \delta / (k_B T) \gg (R_0^2 / (N\delta^2))^{6\nu / (2-3\nu)}$ .

Upon increasing the applied electric field, we enter the last regime where the chains encounter negligible potential barriers, and migrate with the same electrophoretic velocities.

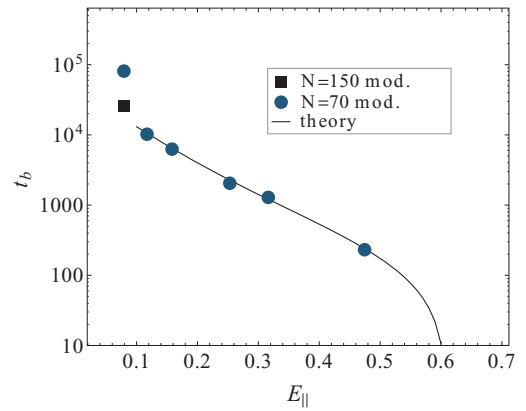


FIG. 11. (Points) Log-linear plot of the trapping time  $t_b$  of the chains in the cavities of the variable diameter cylinder as a function of the applied electric field  $E_{\parallel}$  (not pulse) and (continuous line) scaling prediction from Eq. (16). Only at the lowest field value  $t_b$  could be measured for the chain with  $N = 150$ .

For the chain with  $N = 70$  monomers migrating in modulated cylinders, under constant applied electric field, the trapping times  $t_b$  measured according with the sketch in Fig. 5 are fit with the above Eq. (16) over the middle interval of fields. Considering the various approximations made in the scaling theory (neglect of the charge-charge interactions and the straightening of the rounded shape of the cavities), the agreement with the scaling theory in Fig. 11 appears to be reasonably good. At very high fields, the above scaling of  $\tau = \tau(E_{\parallel})$  predicts a strong decrease with the field. In this regime, the chain mobility approaches a plateau value (Figs. 12 and 13).

In the case of pulse electric fields, a scaling theory can be similarly constructed by taking the weighted average of the above trapping time during the on-time window of the pulse field, with the relaxation time  $\tau_0$  during the off-time window. To estimate  $\tau_0$ , we first notice in Fig. 6 that the motion of the center of mass of the chain during the off-time window of pulse fields is in opposite direction to the direction of motion in the on-time window. This means that the chain, when the field is switched off, is most likely found in a state where it tries to reach the maximum of the potential barrier. The problem is therefore of finding the exit time of the chain from

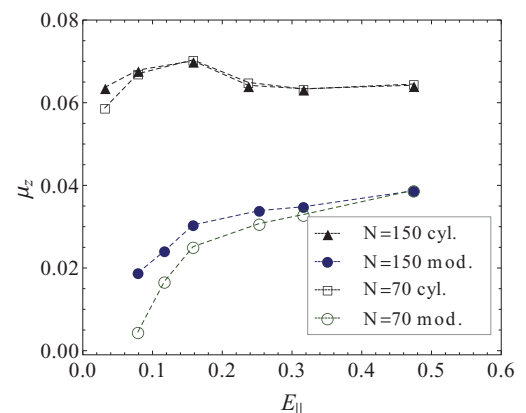


FIG. 12. Electrophoretic mobilities  $\mu_z$  of the chains in straight and variable diameter cylinders as a function of the applied electric field.

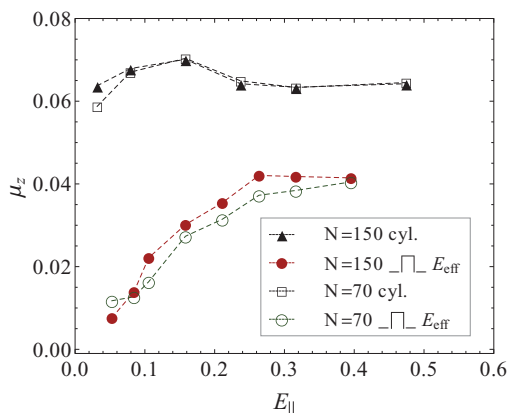


FIG. 13. Electrophoretic mobilities  $\mu_z$  of the chains under applied pulse electric fields  $E_{||}$  in variable diameter cylinders. ( $E_{||}$  is rescaled by a factor of 1/3 to account for the off-time window of the time period.) As a reference, the electrophoretic mobilities  $\mu_z$  of the chains under applied constant electric fields from Fig. 12 are also reproduced here.

inside a connecting channel into a cavity. Assuming that the first monomer/blob of the chain is initially at  $x$  in the interval  $(0, x^*)$  then the mean exit time through the particular end at  $x = 0$  is as follows:<sup>26</sup>

$$\tau_0 \sim \frac{x(2x^* - x)}{3D}, \quad (17)$$

where  $D \sim 1/R_{||}$  is the diffusion constant of a chain with  $N$  monomers.<sup>27</sup> The chain extensions in the axial direction  $R_{||} = |z_{max} - z_{min}|$  are shown in Fig. 8. If we focus on the largest values of  $E_{||}$ , or equivalently  $E_{eff}$ , we notice from Fig. 8 that  $R_{||} \sim N$ . From Eq. (17), it follows that the delay due to relaxation processes, which depends on the depth  $x$  at the time the applied field was switched off, is given by the following relation:

$$\tau_0 \sim x(2x^* - x)N. \quad (18)$$

The probability of exiting through point  $x = 0$  depends on  $x$  and is proportional with  $(x^* - x)/x^*$ .<sup>26</sup> Since the most part of the escape time during the field-on state is spent by the chain trying to reach the maximum of the potential barrier at  $x^*$ , it follows that if the chain just passed the maximum of the potential barrier at  $x^*$ , then during the off-time window of the field it will not retract into the cavity it came from, but simply move forward. However, if the chain is not yet at  $x \rightarrow x^*$  then<sup>26</sup>

$$\tau_0 \sim (x^{*2})N. \quad (19)$$

Considering that  $x^* = A/(2B)$  and  $B = B(E_{||})$  increases with the applied field while  $A = A(E_{||})$  decreases with the field, and here also the trapping time  $t_b$  during the on-time window is almost negligible, independent on  $N$ , it follows from Eq. (19) that the influence of  $\tau_0$  on the electrophoretic velocity becomes negligible and thus independent of  $N$  at very high fields. This trend is eventually observed in Fig. 13 at  $E_{eff} \approx 0.4$ .

## V. CONCLUSIONS

In summary, we performed molecular dynamics simulations of electrophoretic motion of charged chains in classical constant, and variable diameter cylinder geometries. The modulated cylinders are in a sense similar to a series of nanopore constrictions connected by expanding chambers. From these computer experiments, we showed that in constant diameter cylinders, charged chains driven by constant electric fields move with electrophoretic velocities, which quickly become independent of chain length as the field is increased. In modulated geometries (or straight cylinders of variable diameter), the size-separation of charged chains can be achieved with a higher resolution than in constant diameter cylinders if the applied fields are weak. Here, it is important to have in the design expansion chambers that are tailored to the chain sizes that we want to separate. For two chain sizes, the cavities should be large enough to contain the short species, but not the largest. Naturally, the method would not work for chain sizes very close to each other, because of fluctuations.

At high fields, as shown, both constant and variable diameter geometries lead however to velocities independent of  $N$ . A strong coupling between forces due to chain elasticity, diffusion processes, and external potentials, must enter into the description of the problem if faster separation of the charged chains by size is required. We showed that by mixing biased diffusion in modulated geometries and relaxation processes, which in fact amounts to using pulse electric fields, the separability limit, where the chains can still be distinguishable, can be pushed to even higher velocities. Nevertheless, at high fields, the electrophoretic velocities of the chains become once again independent of chain length. This observation leaves the door open for further improvements in electrophoresis of charge chains, particularly, for studies on the effect of the on-off time windows of the pulse electric field, dielectrophoretic effects,<sup>28,29</sup> separability resolution as a function of device parameters, or use of pre-filtration systems.

<sup>1</sup>D. C. Schwartz and C. R. Cantor, "Separation of yeast chromosome-sized DNAs by pulsed field gradient gel electrophoresis," *Cell* **37**, 67–75 (1984).

<sup>2</sup>S. B. Smith, C. Heller, and C. Bustamante, "Model and computer simulations of the motion of DNA molecules during pulse field gel electrophoresis," *Biochemistry* **30**, 5264–5274 (1991).

<sup>3</sup>S. Qian and Y. Ai, *Electrokinetic Particle Transport in Micro-/Nanofluidics: Direct Numerical Simulation Analysis*, Surfactant Science Series (CRC, Taylor & Francis, Boca Raton, USA, 2012), Vol. 153.

<sup>4</sup>G. T. G. Sigalov, J. Comer, and A. Aksimentiev, "Detection of DNA sequences using an alternating electric field in a nanopore capacitor," *Nano Lett.* **8**, 56–63 (2008).

<sup>5</sup>E. Y. N. Laachi, M. Kenward, and K. D. Dorfman, "Force-driven transport through periodic entropy barriers," *Eur. Phys. Lett.* **80**, 50009 (2007).

<sup>6</sup>C. Sathé, X. Zou, J.-P. Leburton, and K. Schulten, "Computational investigation of DNA detection using graphene nanopores," *ACS Nano* **5**, 8842–8851 (2011).

<sup>7</sup>R. Raccis, A. Nikoubashman, M. Retsch, U. Jonas, K. Koynov, H.-J. Butt, C. N. Likos, and G. Fytas, "Confined diffusion in periodic porous nanostructures," *ACS Nano* **5**, 4607–4616 (2011).

<sup>8</sup>K.-H. Paik, Y. Liu, V. Tabard-Cossa, M. J. Waugh, D. E. Huber, J. Provine, R. T. Howe, R. W. Dutton, and R. W. Davis, "Control of DNA capture by nanofluidic transistors," *ACS Nano* **6**, 6767–6775 (2012).

<sup>9</sup>B. Luan, H. Peng, S. Polonsky, S. Rossnagel, G. Stolovitzky, and G. Martyna, "Base-by-base ratcheting of single stranded DNA through a solid-state nanopore," *Phys. Rev. Lett.* **104**, 238103 (2010).

<sup>10</sup>Y. Zhang, J. J. de Pablo, and M. D. Graham, "An immersed boundary method for Brownian dynamics simulation of polymers in complex

- geometries: Application to DNA flowing through a nanoslit with embedded nanopits," *J. Chem. Phys.* **136**, 014901 (2012).
- <sup>11</sup>H. Yong, Y. Wang, S. Yuan, B. Xu, and K. Luo, "Driven polymer translocation through a cylindrical nanochannel: Interplay between channel length and the chain length," *Soft Matter* **8**, 2769–2774 (2012).
- <sup>12</sup>A. G. Oukhaled, A.-L. Biance, J. Pleta, L. Auvray, and L. Bacri, "Transport of long neutral polymers in the semidilute regime through a protein nanopore," *Phys. Rev. Lett.* **108**, 088104 (2012).
- <sup>13</sup>M. Langecker, D. Pedone, F. C. Simmel, and U. Rant, "Electrophoretic time-of-flight measurements of single DNA molecules with two staked nanopores," *ACS Nano Lett.* **11**, 5002–5007 (2011).
- <sup>14</sup>T. N. Shendruk, O. A. Hickey, G. W. Slater, and J. L. Harden, "Electrophoresis: When hydrodynamics matter," *Curr. Opin. Colloid Interface Sci.* **17**, 74–82 (2012).
- <sup>15</sup>S. van Dorp, U. F. Keyser, N. H. Dekker, C. Dekker, and S. G. Lemay, "Origin of the electrophoretic force on DNA in solid-state nanopores," *Nat. Phys.* **5**, 347–351 (2009).
- <sup>16</sup>H.-C. Chang and L. Y. Yeo, *Electrokinetically Driven Microfluidics and Nanofluidics* (Cambridge University Press, New York, 2010).
- <sup>17</sup>M. B. Mikkelsen, W. Reisner, H. Flyvbjerg, and A. Kristensen, "Pressure-driven DNA in nanogroove arrays: Complex dynamics leads to length- and topology-dependent separation," *Nano Lett.* **11**, 1598–1602 (2011).
- <sup>18</sup>J. P. Hernández-Ortiz, M. Chopra, S. Geier, and J. J. de Pablo, "Hydrodynamic effects on the translocation rate of a polymer through a pore," *J. Chem. Phys.* **131**, 044904 (2009).
- <sup>19</sup>A. Milchev, "Single-polymer dynamics under constraints: Scaling theory and computer experiment," *J. Phys.: Condens. Matter* **23**, 103101 (2011).
- <sup>20</sup>G. I. Nixon and G. W. Slater, "Entropic trapping and electrophoretic drift of a polyelectrolyte down a channel with a periodically oscillating width," *Phys. Rev. E* **53**, 4969–4980 (1996).
- <sup>21</sup>M. Tuckerman, *Statistical Mechanics: Theory and Molecular Simulation* (Oxford University Press, New York, 2010).
- <sup>22</sup>M. Rubinstein and R. H. Colby, *Polymer Physics* (Oxford University Press, 2011).
- <sup>23</sup>T. Sakaue, "DNA electrophoresis in designed channels," *Eur. Phys. J. E* **19**, 477–487 (2006).
- <sup>24</sup>N. Nikoofard and H. Fazli, "Free-energy barrier for electric-field-driven polymer entry into nanoscale channels," *Phys. Rev. E* **83**, 050801(R) (2011).
- <sup>25</sup>N. G. V. Kampen, *Stochastic Processes in Physics and Chemistry*, 3rd ed. (Elsevier, Amsterdam, Netherlands, 2007).
- <sup>26</sup>C. Gardiner, *Stochastic Methods: A Handbook for the Natural and Social Sciences*, 4th ed. (Springer-Verlag, Berlin, 2009).
- <sup>27</sup>M. Daoud, "Statistics of macromolecular solutions trapped in small pores," *J. Phys.* **38**, 85–93 (1977).
- <sup>28</sup>A. Y. Grosberg and Y. Rabin, "DNA capture into a nanopore: Interplay of diffusion and electrohydrodynamics," *J. Chem. Phys.* **133**, 165102 (2010).
- <sup>29</sup>H. Morgan and N. G. Green, *AC Electrokinetics: Colloids and Nanoparticles* (Research Studies Press, Baldock, Hertfordshire, England, 2003).